Inorg. Chem. **2005**, *44*, 3738–3745

Kinetic and Thermodynamic Characterization of the Cobalt and Manganese Oxyhydroxide Cores Formed in Horse Spleen Ferritin

Bo Zhang,[||] John N. Harb,[†] Robert C. Davis,[‡] Jae-Woo Kim,[§] Sang-Hyon Chu,[§] Sang Choi,[§] Tim Miller,[†] and Gerald D. Watt*[,||]

Departments of Chemistry and Biochemistry, Chemical Engineering, and Physics, Brigham Young University, Provo, Utah 84602, and NASA Langley Research Center, Hampton, Virginia 23681

Received July 9, 2004

Horse spleen ferritin (HoSF) containing 800–1500 cobalt or 250–1200 manganese atoms as Co(O)OH and Mn(O)OH mineral cores within the HoSF interior (Co–HoSF and Mn–HoSF) was synthesized, and the chemical reactivity, kinetics of reduction, and the reduction potentials were measured. Microcoulometric and chemical reduction of HoSF containing the M(O)OH mineral core (M = Co or Mn) was rapid and quantitative with a reduction stoichiometry of 1.05 ± 0.10 e/M forming a stable $M(OH)_2$ mineral core. At pH 9.0, ascorbic acid (AH_2), a two-electron reductant, effectively reduced the mineral cores; however, the reaction was incomplete and rapidly reached equilibrium. The addition of excess AH_2 shifted the reaction to completion with a M^{3+}/AH_2 stoichiometry of 1.9–2.1, consistent with a single electron per metal atom reduction. The rate of reaction between M(O)OH and excess AH_2 was measured by monitoring the decrease in mineral core absorbance with time. The reaction was first order in each reactant with second-order rate constants of 0.53 and 4.74 M^{-1} min^{-1}, respectively, for Co– and Mn–HoSF at pH 9.0. From the variation of absorbance with increasing AH_2 concentration, equilibrium constants at pH 9.0 of 5.0 ± 1.9 for Co–HoSF and 2.9 ± 0.9 for Mn–HoSF were calculated for $2M(O)OH + AH_2 = 2M(OH)_2 + D$, where AH_2 and D are ascorbic acid and dehydroascorbic acid, respectively. Consistent with these equilibrium constants, the standard potential for the reduction of Co(III)–HoSF is 42 mV more positive than that of the ascorbic acid reaction, while the standard potential of Mn(III)–HoSF is 27 mV positive relative to AH_2. Fe^{2+} in solution with Co– and Mn–HoSF under anaerobic conditions was oxidized to form Fe(O)OH within the HoSF interior, resulting in partial displacement of the Co or Mn by iron.

Introduction

Ferritins are naturally occurring iron storage biomolecules involved in maintaining iron availability for cellular metabolism as well as sequestering free iron and preventing deleterious radical formation. Most ferritins from plants, animals, and bacteria share a common structure consisting of 24 subunits arranged with 432 symmetry to form nearly spherical molecules 12 nm in overall diameter with hollow interiors 8 nm in diameter.[1−6] A ferritin-like protein recently isolated from bacteria *Listeria innocua* is atypical compared to the majority of structurally characterized ferritins.[7] It is composed of 12 identical 18 kDa subunits, which self-assemble into an empty cage having 23 symmetry. The arrangement of the subunits forms 3- and 4-fold channels that are ∼0.40 nm in diameter that connect the interior cavity with the exterior solution, through which ions transit the protein shell. Naturally occurring cores in both animal and bacterial ferritins contain iron(III), as well as some phosphate. The nature of the cores, however, is different. The interior

* To whom correspondence should be addressed: Telephone: (801) 422-4561. Fax: (801) 422-5474. E-mail: gdwatt@chem.byu.edu.
[||] Department of Chemistry and Biochemistry, Brigham Young University.
[†] Department of Chemical Engineering, Brigham Young University.
[‡] Department of Physics, Brigham Young University.
[§] NASA Langley Research Center, Hampton, VA 23681.

(1) Theil, E. C. *Annu. Rev. Biochem.* **1987**, *56*, 289−316.
(2) Harrison, P. M.; Arosio, P. *Biochim. Biophys. Acta* **1996**, *1275*, 161−203.
(3) Proulx-Curry, P. M.; Chasteen, N. D. *Coord. Chem. Rev.* **1995**, *144*, 347−368.
(4) Crichton, R. R.; Charloteaux-Wauters, M. *Eur. J. Biochem.* **1987**, *164*, 485−506.
(5) Rice, D. W.; Ford, G. C.; White, J. L.; Smith, J. M. A.; Harrison, P. M. *Adv. Inorg. Biochem.* **1983**, *5*, 39−50.
(6) Ford, G. C.; Harrison, P. M.; Rice, D. W.; Smith, J. M. A.; Treffry, A.; White, J. L.; Yariv, J. *Philos. Trans. R. Soc. London, Ser. B* **1984**, *304*, 551−566.
(7) Bozzi, M.; Mignogna, G.; Stefanini, S.; Barra, D.; Longhi, C.; Valenti, P.; Chiancone, E. *J. Biol. Chem.* **1997**, *272*, 3259−3265.

10.1021/ic049085l CCC: $30.25
Published on Web 04/12/2005

cavity of animal ferritin naturally contains an iron oxyhydroxide mineral core consisting of 2000−3000 iron atoms, whereas, bacterial ferritins typically contain a phosphohydroxy mineral core of similar size.[8,9] The mineral core of ferritins is easily removed by reduction and chelation to form apo ferritin; it is also readily reconstituted by adding Fe^{2+} to apo ferritin in the presence of an oxidant, which is commonly O_2 from air. The protein itself is known not to undergo oxidation or deactivation by oxidants such as O_2 or H_2O_2.[10,11]

Because of the unique template structure of apo ferritin, a variety of new, nonbiological mineral cores have been synthesized and characterized within the apo ferritin interior.[12−19] These new ferritin cores range from Co(O)OH,[12,13] Mn(O)OH,[14−16] magnetite,[17] and Ni and Cr nanoparticles,[18] all bearing a resemblance to native ferritin cores, to mineral cores containing technologically interesting materials such as CdS.[19] Electron microscopic evidence showed that these new materials formed exclusively and quantitatively within the ferritin interior.[12−16] This is remarkable because many of the reagents used to form these new ferritin mineral cores are expected to react upon mixing to form insoluble precipitates. The failure to form the expected precipitates suggests that ferritin has precise mechanistic control in directing the reagents into its hollow interior.

Earlier studies showed that the native iron mineral cores of both bacterial and animal ferritins could be rapidly and reversibly reduced at potentials of −250 to −420 mV and that, in the absence of chelators, the reduced mineral cores were stable.[8,20] The synthesis of ferritin containing M(O)OH mineral cores (M = Co and Mn) is of interest because it provides an opportunity to compare the thermodynamics and reduction kinetics of M(O)OH with those of ferritin containing the native Fe(O)OH mineral core. The stability of the reduction product will also be determined, as was previously done for $Fe(OH)_2$.[8,20] Such comparisons are of interest in describing the properties of new materials and will aid in understanding the role of the ferritin protein shell in stabilizing the mineral core. The fundamental insights gained from this study will help provide a basis for development of a synthetic protocol to construct more complex and varied mineral cores.

Experimental Section

Horse spleen apo ferritin (HoSF)[21] was prepared by the reductive dissolution of native iron oxide cores of holo HoSF (Sigma) using the thioglycollic acid procedure.[22] Apo HoSF was further reacted with dithionite in the presence of bipyridine to remove iron to <1.0 Fe/HoSF. Protein concentrations were determined by the Lowry method and confirmed by the absorbance at 280 nm (ϵ = 468 000 M^{-1} cm^{-1}).[9] Reactions or procedures requiring anaerobic conditions were carried out in a Vacuum Atmosphere glovebox (<0.5 ppm O_2, Nyad oxygen sensor). Aqueous Fe^{2+} (0.0075 M $FeSO_4$ in 0.001 N HCl) and ascorbic acid (5 mM) stock solutions were stored in the glovebox prior to use. AH_2 was standardized against an $Fe(CN)_6^{3-}$ standard solution by monitoring optically the disappearance of the yellow color of $Fe(CN)_6^{3-}$ (ϵ_{420} = 1020 M^{-1} cm^{-1}) upon reduction to $Fe(CN)_6^{4-}$ by AH_2 ($2[Fe(CN)_6]^{3-} + AH_2 = 2[Fe(CN)_6]^{4-} + D + 2H^+$).

Sample Preparation and Characterization. Cobalt and manganese oxyhydroxide mineral cores were synthesized within the HoSF interior (Co−HoSF and Mn−HoSF, respectively) using procedures previously described.[12,16] The procedure from ref 12 was modified by adding aliquots of $CoSO_4$ (0.025 M, 80 μL) and H_2O_2 (3%, 40 μL) to apo HoSF solution (10^{-5} mmol, 5.0 mL), pH 8.5 in 0.025 M MOPS and 0.05 M NaCl with 15 min intervals between additions. The pH was kept at 8.5−9.0 with 0.1 M NaOH after each addition. The use of MOPS at this pH decreased nonspecific Co(O)OH formation and gave better yields of Co−HoSF. Deposition of Mn(O)OH in HoSF was conducted by addition of aliquots of $MnCl_2$ (0.03 M, 0.5 mL) to apo HoSF (10^{-5} mmol, 5.0 mL) in AMPSO buffer (0.05 M, 0.05 M NaCl, pH 8.9) with air as the oxidant. The reaction was allowed to precede at room temperature over 24 h with stirring.

After synthesis, both Co− and Mn−HoSF solutions were centrifuged to remove any precipitated M(O)OH (little was found at M/HoSF < 1500), and then centrifuged with a 100 kDa membrane in a Nanosep microconcentrator (Pall Gelman Laboratory) that retained the M(O)OH protein species but removed small solution components. The resulting Co−HoSF was shown by transmission electron microscopy (TEM, Figure 1a,b) to have mineral particles within the ferritin interiors as previously described.[12,16] Similar results were observed for Mn−HoSF. Apo HoSF and Co− and Mn−HoSF were passed through a calibrated G-25 Sephadex column (1 cm × 16.5 cm) and exhibited identical elution profiles (Figure 1d), indicating that the structure of the protein cage remained unaltered by the synthesis as previously reported.[12,16] The metal content of the cobalt− and manganese−ferritins was determined after G-25 Sephadex chromatography using an inductively coupled plasma spectrometer (ICP-AES, Perkin-Elmer Optima 2000), and >95% of the metal was found within the protein fraction. All ferritin solutions were stored at 4 °C after synthesis and characterization. Optical spectra of Co−HoSF prepared in MOPS and AMPSO were recorded on a Hewlett-Packard 8453 UV−vis spectrometer. All experiments were done at ~23 °C. Mn− and Co−HoSF and apo HoSF prepared from them

(8) Watt, G. D.; Frankel, R. B.; Papaeftheymiou, G. C.; Spartalian, K.; Stiefel, E. I. *Biochemistry* **1986**, *25*, 4330−4336.
(9) Stiefel, E. I.; Watt, G. D. *Nature* **1979**, *279*, 81−83.
(10) Zhao, G.; Bou-Abdallah, F.; Yang, X.; Arosio, P.; Chasteen, N. D. *Biochemistry* **2001**, *40*, 10832−10838.
(11) Lindsay, S.; Brosnahan, D.; Lowery, T. J., Jr.; Crawford, K.; Watt, G. D. *Biochim. Biophys. Acta* **2003**, *1621*, 57−66.
(12) Douglas, T.; Stark, V. T. *Inorg. Chem.* **2000**, *39*, 1828−1830.
(13) Allen, M.; Willits, D.; Young, M.; Douglas, T. *Inorg. Chem.* **2003**, *42*, 6300−6305.
(14) Meldrum, F. C.; Vanessa, J. W.; Nimmo, D. L.; Heywood, B. R.; Mann. S. *Nature* **1991**, *349*, 684−687.
(15) Mackle, P.; Charnock, J. M.; Garner, C. D.; Meldrum F. C.; Mann. S. *J. Am. Chem. Soc.* **1993**, *115*, 8471−8472.
(16) Meldrum, F. C.; Douglas, T.; Levi, S.; Arosio, P.; Mann, S. *J. Inorg. Biochem.* **1995**, *58*, 59−68.
(17) Meldrum, F. C.; Heywood, B. R.; Mann. S. *Science* **1992**, *257*, 522−523.
(18) Okuda, M.; Iwahori, K.; Yamashita, I.; Yoshimura, H. *Biotechnol. Bioeng.* **2003**, *84*, 187−194.
(19) Wong, K. K. W.; Mann. S. *Adv. Mater.* **1996**, *8*, 928−931.
(20) Watt, G. D.; Jacobs, D.; Frankel, R. B. *Proc. Natl. Acad. Sci. U.S.A.* **1988**, *85*, 7457−7461.

(21) Abbreviations: HoSF, horse spleen ferritin; Co−HoSF and Mn−HoSF, HoSF containing Co(O)OH and Mn(O)OH mineral cores, respectively; AH_2, ascorbic acid; D, dehydroascorbic acid; MOPS, 4-morpholine−propanesulfonic acid; AMPSO, 3-[(1,1-dimethyl-2-hydroxyethyl)-amino]-2-hydroxypropanesulfonic acid; ophen, *o*-phenanthroline; TEM, transmission electron microscopy.

(22) Treffry, A.; Harrison, P. M. *Biochem. J.* **1978**, *171*, 313−320.

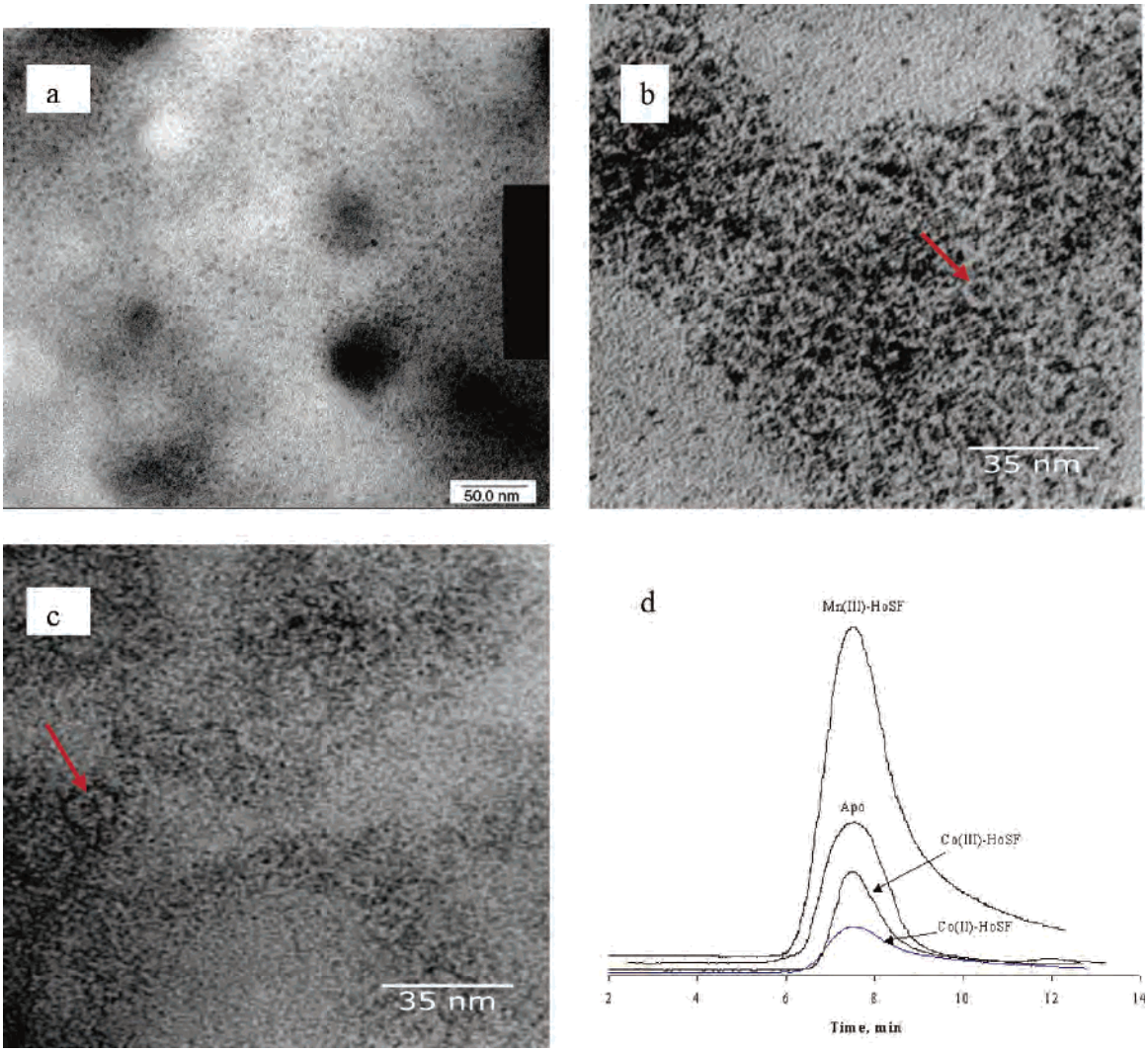

Figure 1. (a) Unstained TEM of Co(O)OH−HoSF containing ~1200 Co atoms; (b) TEM of Co(O)OH−HoSF negatively stained with uranyl acetate; (c) TEM of $Co(OH)_2$−HoSF negatively stained with uranyl acetate; (d) size exclusion chromatography of apo HoSF and Co(O)OH−, Mn(O)OH−, and $Co(OH)_2$−HoSF on a 1 cm × 16.5 cm Sephadex G-25 column measuring absorbance at 280 nm.

were fully active toward Fe^{2+} deposition, demonstrating that the formation of these nonnative mineral cores did not affect the activity of the protein toward iron.

Kinetic Measurements. The kinetics of Co−HoSF reduction by AH_2 was monitored by UV−visible spectrophotometry at pH 9.0 for core sizes ranging from 800 to 1200 Co/HoSF. The initial AH_2 concentration was kept constant and was in at least a 10-fold excess. For 1100 Co/HoSF, aliquots of Co−HoSF ([Co] = 4.06 mM, [Co−HoSF] = 3.67 μM) were added to 1 mL of MOPS buffer (0.025 M at pH 9.0 with 0.05 M NaCl), and the optical spectra were taken to determine the extinction coefficient of Co(III)−HoSF at 350 nm. Then, excess AH_2 (70 μL, 5 mM) was added, and the decreasing absorbance at 350 nm due to reduction of the mineral core was recorded as a function of time. The reduction was typically completed in 10 min. The final absorbance (350 nm) was assumed to be due to Co(II)−HoSF, consistent with pH and coulometric measurements (see below).

The reduction kinetics of Mn(III)−HoSF by AH_2 for core sizes ranging from 250 to 1000 were measured using an Applied Photophysics stopped-flow kinetic instrument. This instrument was preferred over the procedure used for measurement of the Co(III)−HoSF kinetics because of the faster reaction rate of the Mn(III)−HoSF. Measurements for Mn(III)−HoSF performed with both procedures yielded equivalent results. For ~1000 Mn/HoSF, 10, 15, 20, and 30 μL of Mn−HoSF ([Mn] = 4.07 mM, [Mn−HoSF] = 4.1 μM) were diluted to 1 mL with MOPS or AMPSO buffer, pH 9.0, and placed in one stopped-flow syringe. In the other syringe was placed 0.1 mL of AH_2 (5 mM) and 0.9 mL of buffer. After thermal equilibrium was reached, the solutions were mixed and the change in absorbance at 450 nm, the wavelength where Mn(O)OH absorbs,[16] was recorded against time.

Optical titrations of both Co− and Mn−HoSF with AH_2 were performed with an HP 8453 UV−visible spectrometer using a 1.0 cm quartz optical cell. Aliquots of AH_2 solution (5 μL, 5 mM) were added to AMPSO buffered (pH 9.0) Co− or Mn−HoSF solution at 15 or 5 min intervals (Mn−HoSF reacts faster; see Figure 4) until AH_2 was in excess. Stable absorbance values at either 350 or 450 nm were recorded before the next addition.

Bracketing the Reduction Potential. To bracket the reduction potential of M−HoSF (M = Co or Mn), excess reductants with different redox potentials were mixed with M−HoSF solution at ~5 μM, and the reaction was monitored optically at 350 or 450 nm to determine the extent of M−HoSF reduction. The reductants included sodium dithionite (−520 mV), methyl viologen (−440 mV), flavin mononucleotide (−100 mV), methylene blue (0 mV), AH_2 (50 mV), and ferrocyanide (250 mV), where the potentials

are relative to a NHE and pH 7.0 has been assumed for pH-dependent reactions.

Microcoulometry. Microcoulometry was conducted using previously described methods.[23,24] Co−HoSF and Mn−HoSF solutions were first made anaerobic by several evacuation−flush cycles using N_2 and then reduced at pH 8.0 using various viologens at potentials from −200 to −520 mV.

Assessment of M(II)−HoSF Stability. Excess AH_2 was added to a M−HoSF solution (M = Co or Mn) buffered at pH 9.0, and the reaction was allowed to completely reduce the mineral cores (15 min). The reduced solutions were centrifuged to remove any precipitate (none was observed), and then the solution was passed through an anaerobic G-25 column equilibrated with MOPS buffer to isolate the protein fraction and to remove excess AH_2, dehydroascorbic acid (D), and any M^{2+} released by the reduction process. The emerging protein fraction was analyzed for protein and Co or Mn, and the results were compared to the amount of these metals added as Co−HoSF and Mn−HoSF. The reduced Co(II) cores were stable in the HoSF interior and eluted identically with apo HoSF and Co(III)−HoSF (Figure 1c,d). To further establish that the reduced species remained within the HoSF interior, the solution was also centrifuged with a Nanosep microconcentrator containing a 100 kDa membrane to remove any small molecules released by the reaction and to retain the protein fraction and its associated mineral core. The filtrate and the retentate were separately analyzed for Co and Mn by ICP to determine the fraction in which the metals were found. Finally, TEM images of the reduced Co(II)− or Mn-(II)−HoSF were obtained by reducing M(III)−HoSF with excess AH_2, putting the solution on a carbon grid in a vacuum atmosphere glovebox and negatively staining with uranyl acetate.

Reaction of M−HoSF with Fe(II). Iron deposition into Co−HoSF was conducted anaerobically in a glovebox by adding Fe^{2+} to newly made Co−HoSF solution (3.97 mM Co, 4.3 μM HoSF, ~920 Co/HoSF) at Fe/Co ratios of 0−2.0. At 30 s intervals, 0.2 mL of the mixed solutions was withdrawn and added to 1 mL of ophen in MOPS buffer. The unreacted Fe^{2+} was determined as $[Fe(ophen)_3]^{2+}$ at 511 nm (ϵ_{511} = 9640 M^{-1} cm^{-1}). The amount of Fe^{2+} oxidized was determined from these measurements, and then the solution was filtered through a Nanosep microconcentrator containing a 100 kDa membrane. The emerging and retained solutions were analyzed for iron and cobalt with ICP-AES. For Mn−HoSF, similar experiments were conducted for ~1:1 ratio of Fe/Mn.

Results

The formation of Co(O)OH with 800−2000 Co/HoSF within the HoSF interior was conducted in MOPS and AMPSO buffers at pH 8.5−9.0 using H_2O_2 as the oxidant.[12] Figure 1 verifies by TEM that the oxidized mineral cores were within the ferritin interior as previously reported.[12−16] Figure 1 also shows that the reduced mineral core was present in the HoSF interior as previously established for the Fe-$(OH)_2$ mineral cores.[20] Core formation was observed to depend on the choice of solution buffer. Only small cores that were faintly purple in color were produced in Tris buffer. In contrast, larger stable cores were formed in MOPS and AMPSO buffers under the same conditions where the solution was observed to turn brown upon Co(II) addition. As the cores approached ~2000 Co atoms, nonspecific Co-(O)OH formation occurred outside the HoSF interior and contributed to protein precipitation. The amount of nonspecific Co(O)OH formation decreased with the use of smaller aliquots of Co^{2+}, which presumably compensated for the decreased rate of Co incorporation into the protein at higher loadings. However, use of smaller aliquots significantly slowed the synthesis process.

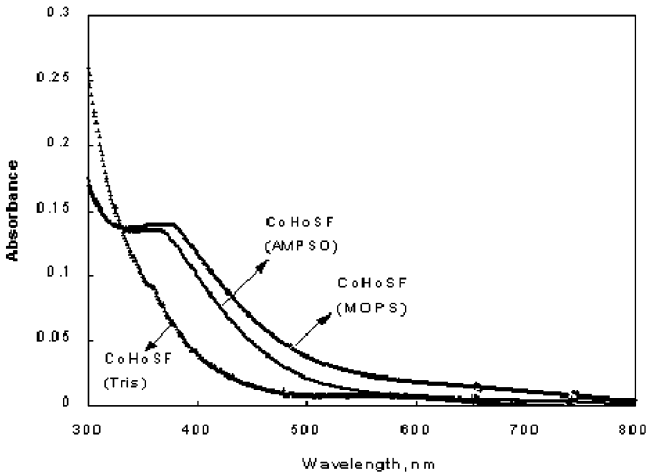

Figure 2. Optical spectra of Co−HoSF at the same Co concentration of 0.062 mM for Co−HoSF prepared in MOPS, Tris, and AMPSO at pH 8.5. The Co−HoSF samples prepared in MOPS and AMPSO contained 1000 Co/HoSF, but because of the instability of the Co mineral core formed in Tris, that sample contained only ~200 Co/HoSF.

In addition to variation in mineral core size, each buffer produced a mineral core with different optical properties, as shown in Figure 2, all taken at the same Co concentration. The three Co−HoSF species have different spectra, indicating that the mineral cores differ from one another, with that prepared in Tris buffer differing most. The spectra of Co−HoSF prepared in MOPS and AMPSO are consistent with reported results (Figure 1 in ref 12 and Figure 3 in ref 13). The broad absorption centered at 350 nm (Figure 2) is consistent with a O → Co(III) charge-transfer band in Co-(O)OH.[25] In contrast, apo HoSF prior to mineralization showed no absorption at 350 nm. When allowed to incubate at 4 °C for several days, the sample prepared in Tris was the least stable, as small amounts of Co(O)OH began to precipitate upon standing. In contrast, samples prepared in MOPS and AMPSO remained stable for months. After centrifuging with a 100 kDa membrane, >98% of the Co remained with HoSF prepared in MOPS and AMPSO, while only ~20% remained when prepared in Tris. For these reasons, Co−HoSF prepared in Tris was not used for experiments in the current study, although the observed buffer-related effects are the object of continuing investigation.

Chemical Reduction of Co and Mn−HoSF. After preparation, Co−HoSF was made anaerobic and reduced coulometrically at pH 8.0 using various viologens as mediators at potentials from −200 to −520 mV. Reduction was

(23) Watt G. D.; Frankel R. B. In *Iron Biominerals*; Plenum Press: New York, 1991; pp 307−313.
(24) Watt R. K.; Frankel R. B.; Watt G. D. *Biochemistry* **1992**, *31*, 9673−9679.
(25) Dimitrou, K.; Brown, A. D.; Folting, K.; Christou, G. *Inorg. Chem.* **1999**, *38*, 1834−1841.

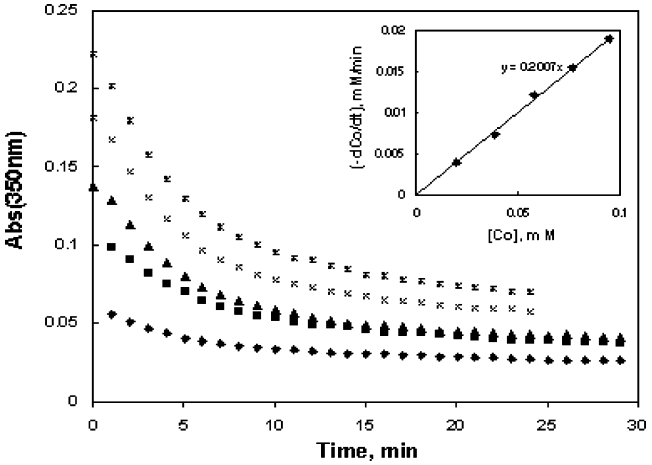

Figure 3. Time-resolved changes in the optical absorption at 350 nm after mixing Co−HoSF ([Co] = 4.06 mM, [HoSF] = 3.67 μM, ~1100 Co/HoSF) and AH_2. The conditions were [AH_2] = 0.35 mM; [Co(III)] = 0.02, 0.04, 0.058, 0.077, and 0.095 mM (from bottom to top); 0.025 M MOPS; and 0.05 M NaCl, pH 9.0 The insert shows the Co(III) concentration dependence of the reduction of Co−HoSF with AH_2.

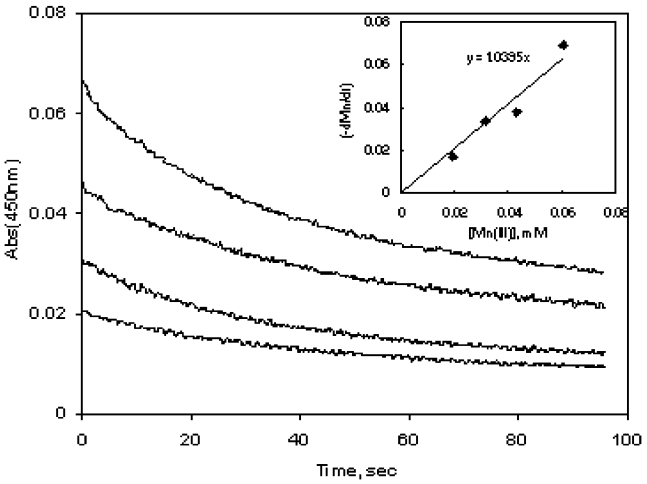

Figure 4. Time-resolved changes in the absorption at 450 nm after mixing Mn−HoSF ([Mn] = 4.07 mM, [HoSF] = 4.1 μM, ~1000 Mn/HoSF) and AH_2. The conditions were [AH_2] = 0.24 mM; [Mn(III)] = 0.02, 0.032, 0.043, and 0.06 mM (from bottom to top); 0.025 M MOPS; and 0.05 M NaCl, pH 9.0. The insert shows the Mn(III) concentration dependence of the reduction of Mn−HoSF with AH_2.

complete upon mixing with a stoichiometry of 1.05 ± 0.10 e/Co over this voltage range, indicating that Co(III) was initially present and was quantitatively reduced to Co(II). These results also established that the reduction potential for the Co−HoSF mineral core is more positive than −200 mV for

$$\text{Co(III)}-\text{HoSF} + \text{H}_2\text{O} + \text{e} = \text{Co(II)}-\text{HoSF} + \text{OH}^- \quad (1)$$

To more closely define the reduction potential for (1), Co−HoSF was reacted with reduced flavin mononucleotide ($FMNH_2$, −100 mV) and methylene blue (MBH_2, ~0 mV). Consistent with the coulometric results using viologen mediators, $FMNH_2$ readily reduced the mineral core, but MBH_2 was only marginally effective. These results suggest a redox potential for the Co(III)−HoSF near 0 mV, a conclusion supported by experiments using ascorbic acid (AH_2, +50 mV), which conveniently reduces both Co− and Mn−HoSF in an equilibrium reaction. Detailed kinetic and thermodynamic studies were undertaken with AH_2 as reported below.

Kinetics of Co− and Mn−HoSF Reduction. Figure 3 shows the reaction of Co−HoSF at various concentrations with excess AH_2 at pH 9.0. Although MOPS is not a good buffer at pH 9.0 (pK_a = 7.2), the overall reaction, summarized by reaction 2, indicates the reaction does not change the pH, where M = Co or Mn, and AH_2 and D are ascorbic acid and dehydroascorbic acid, respectively. MOPS was used for convenience because Co−HoSF was initially prepared in this buffer. Identical results were obtained in AMPSO (pK_a = 9.0).

$$2\text{M(III)}-\text{HoSF} + \text{AH}_2 = 2\text{M(II)}-\text{HoSF} + \text{D} \quad (2)$$

The inset to Figure 3 shows that the rate of Co(III)−HoSF reduction increased linearly with increasing Co−HoSF concentration, suggesting a first-order reaction. A similar first-order dependence of the rate with varying AH_2 concentration was also observed (data not shown). The overall second-order rate constant calculated from duplicate measurements was 0.53 ± 0.03 M^{-1} min^{-1}. While the reduction rate of Co−HoSF with AH_2 was easily measured, it was not as rapid as with the viologens and required several minutes for completion.

As shown by the stopped-flow traces in Figure 4, the rate of Mn−HoSF reduction under the same conditions as Co−HoSF for a core size of 1000 Mn/HoSF increased linearly with increasing Mn−HoSF concentration when the AH_2 concentration was kept constant and in large excess. Similar behavior was noted for a core size of 250, suggesting that the rate was invariant with core loading.[26] The rate was also first order in AH_2. A second-order rate constant of 4.74 ± 0.08 M^{-1} min^{-1} for the reduction of Mn(III)−HoSF by AH_2 was determined. Thus, the rate of Mn−HoSF reduction with AH_2 was about 10 times faster than that of Co−HoSF under the same conditions.

Reduction of Co−HoSF and Mn−HoSF. The equilibrium titrations in Figures 5 and 6 show the optical spectra of the Co− and Mn−HoSF as AH_2 was added incrementally and allowed to fully react. The absorbances associated with the Co(III)−HoSF and Mn(III)−HoSF mineral cores both decreased nonlinearly (in separate experiments) and eventually reached a limiting value as equilibrium was approached (see reaction 2).

The stoichiometry of these reactions was established by adding known amounts of AH_2 to either Co− or Mn−HoSF, allowing the reaction to reach equilibrium, making the solution anaerobic, and then measuring the amount of unreacted M(III)−HoSF remaining by microcoulometry. D is electrochemically inactive under anaerobic conditions.

(26) Before kinetic and thermodynamic measurements, TEM measurements for both Co(OOH) and Mn(OOH) indicated that the mineral cores were within the ferritin interiors, and, for both compounds, a distribution of cores was observed as previously described using TEM.[12−14] The kinetic and thermodynamic results reported here arise from reactions of this heterogeneous population of mineral cores but remained constant with average core size variation.

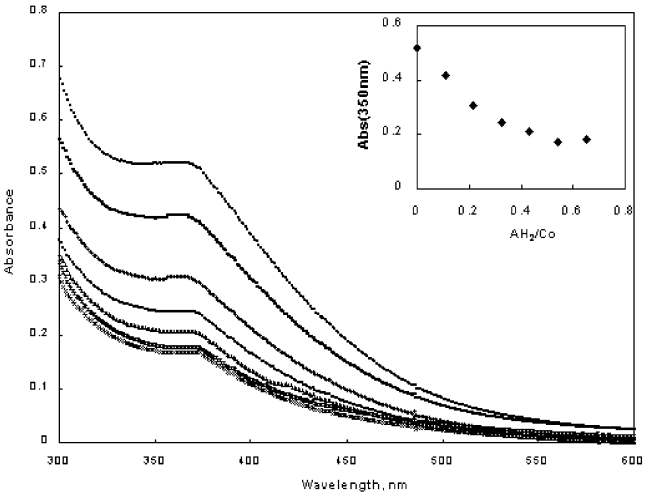

Figure 5. Optical titration of Co(III)−HoSF with AH_2. The spectra were taken every 15 min after adding 5 μL of 5 mM AH_2 to 0.24 mM Co(III)−HoSF ([HoSF] = 0.22 μM) in 1 mL of AMPSO buffer (0.025 M with 0.05 M NaCl, pH 9.0). The insert shows that the absorbance at 350 nm decreases with AH_2 addition until it becomes stable when all Co(III)−HoSF is reduced to Co(II)−HoSF. At the equivalence point, ~1.8 Co(III) is reduced for each AH_2 added.

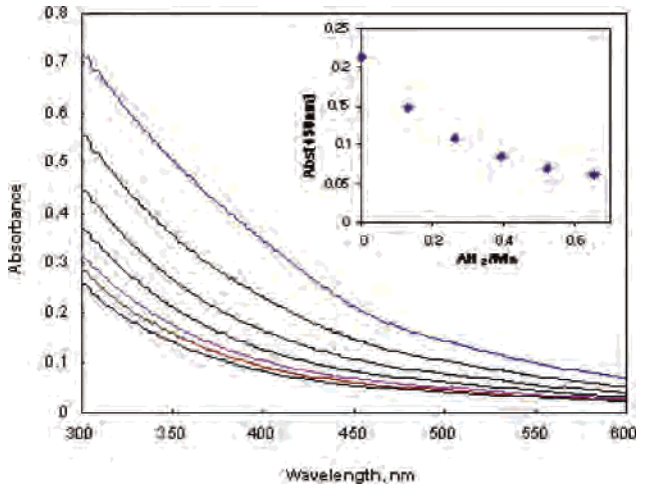

Figure 6. Optical titration of Mn(III)−HoSF with AH_2. The spectra were taken every 15 min after adding 5 μL of 5 mM AH_2 to 0.20 mM Mn(III)−HoSF ([HoSF] = 0.20 μM) in 1 mL of AMPSO buffer (0.025 M with 0.05 M NaCl, pH 9.0). The insert shows that the absorbance at 450 nm decreases with AH_2 addition until it becomes stable when all Mn(III)−HoSF is reduced to Mn(II)−HoSF. At the equivalence point, ~1.9 Mn(III) is reduced for each AH_2 added.

From the initial points of the curve in the inset, the stoichiometry of 1.85−2.10 M/AH_2 was determined. When M−HoSF was reduced with AH_2 at pH 9.0, no change in pH was observed in accordance with reaction 2. These measurements establish that the reduction of both Co− and Mn−HoSF occurs by a single electron reaction. This result, together with a knowledge of the structure of the oxidized core,[12−16] indicates that $M(OH)_2$ is the product of M(O)OH reduction and that the limiting spectrum in Figures 5 and 6 at high AH_2 concentrations corresponds to that of ferritin containing the $M(OH)_2$ mineral core. The molar absorptivity of the $Co(OH)_2$ mineral core at 350 nm was calculated to be 976 ± 73 M^{-1} cm^{-1}. That for $Mn(OH)_2$ at 450 nm was 348 ± 61 M^{-1} cm^{-1}.

The fact that the reduced species remained inside the core was confirmed by adding excess AH_2 to Co−HoSF, allowing the reaction to reach equilibrium and then either centrifuging the HoSF containing the $Co(OH)_2$ mineral core with a Nanosep centrifuge tube containing a 100 kDa membrane or conducting gel filtration on a G-25 column. No precipitate of $Co(OH)_2$ was observed in the initial solution upon reduction with AH_2, little Co^{2+} passed through the membrane, and about 85−90% Co(II) was found associated with the HoSF fraction retained in the centrifuge tube. G-25 Sephadex gel filtration of the AH_2-reduced solution produced an elution profile in Figure 1d, indicating the protein with the reduced core eluted as native HoSF. These results suggest that $Co(OH)_2$ is strongly associated with the protein and likely inside the HoSF interior. The presence of a core in Co(II)−HoSF was confirmed by TEM (Figure 1c). Similar experiments were conducted with Mn−HoSF, and the $Mn(OH)_2$ was also bound as a mineral core.

Thermodynamics of Co− and Mn−HoSF Reduction. From the insert in Figure 5 and from the measurement of Co(III)−HoSF concentrations by microcoulometry at various AH_2 concentrations, an equilibrium constant of 5.0 ± 1.9 was determined for reaction 2, where M = Co. Measurements were made at pH 9. Curve fitting of the optical titration data is shown in Figure 1 of the Supporting Information. Similar experiments conducted for Mn−HoSF resulted in an equilibrium constant of 2.9 ± 0.9 for reaction 2, where M = Mn. Consistent with these equilibrium constants, the standard potentials for the reduction of Co(III)−HoSF and Mn(III)−HoSF are 42 and 27 mV, respectively, more positive than that of the ascorbic acid reaction.

Reaction of M−HoSF with Fe^{2+}. The reaction of Fe^{2+} with Co−HoSF was conducted anaerobically to determine if the contained but oxidized Co(O)OH mineral core would react with Fe^{2+} and, if so, to determine the fate of the Fe(O)OH and $Co(OH)_2$ products. Anaerobic conditions assured that the Co(O)OH mineral core was the only oxidant present. Upon the addition of small aliquots of Fe^{2+} (0−1 Fe^{2+}/Co^{3+}), Fe^{2+} was readily oxidized as evidenced by the lack of $[Fe(ophen)_3]^{2+}$ formation upon addition of excess ophen; however, no external Fe(O)OH precipitate was evident, suggesting that iron was deposited within the ferritin interior. This hypothesis was verified by analysis, which found the added iron associated with the HoSF fraction. The amount of Co(II) associated with the protein was determined by ICP after centrifuging the reaction mixture through a 100 kDa membrane contained in a Nanosep microconcentrator or following G-25 Sephadex chromatography. Figure 7 shows that the amount of Co associated with the HoSF decreased as iron was deposited, indicating the release of Co from the core. The most probable explanation for this observation is that Fe^{2+} is oxidized by the Co(O)OH mineral core forming Fe(O)OH and releasing Co(II). However, ~20% of the cobalt remained associated with HoSF, even at Fe^{2+}/Co^{3+} ratios > 1:1. Similar results were obtained for Mn−HoSF at an ~1:1 Fe^{2+}/Mn^{3+} ratio with about 30% Mn remaining inside. It is possible that a volume limitation is reached as iron is added, leading to the release of the less stable $M(OH)_2$. Another

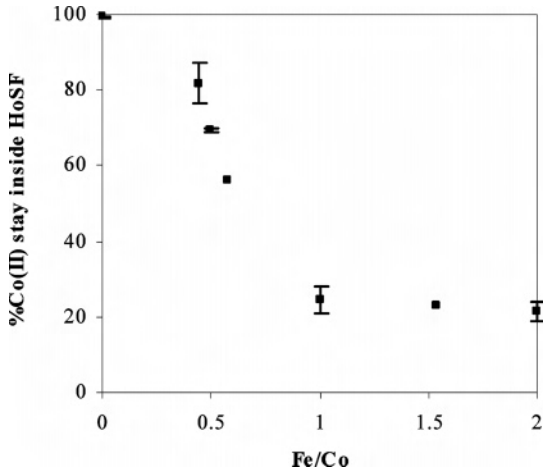

Figure 7. Reaction of Co(III)−HoSF and Fe^{2+} under anaerobic conditions at pH 8.5 and 0.05 M MOPS buffer, showing the percent of Co(II) present within HoSF as a function of Fe^{2+} concentration. Aliquots of Fe^{2+} were added to Co(III)−HoSF solution (3.97 μM Co, 4.3 μM HoSF, ~920 Co/HoSF) so that Fe/Co = 0, 0.44, 0.58, 1.0, and 2.0. Cobalt concentrations were determined by ICP-AES after centrifuging through a 100 kDa membrane.

possibility is that $M(OH)_2$ is initially formed on the surface of M(O)OH when Fe^{2+} makes surface contact, but the more stable Fe(O)OH prevents the less stable $M(OH)_2$ from forming a stable bulk phase, which, by itself, is stable within the ferritin interior as shown above.

Discussion

The use of supermolecular protein cages of HoSF for synthesis of inorganic materials of nanometer size has been a recent and important research theme, and a wide variety of mineral cores have been produced.[12−19] Three general types of reactivity have been employed to create new core materials: (1) chemical in situ transformation of the native ferritin iron oxide mineral core, (2) reconstitution of apo ferritin molecules with redox-active metal ions, and (3) hydrolytic polymerization within the mineral core. Recently a new route for obtaining nanoparticles of Prussian blue in HoSF was developed using a denature−renature method.[27] Reconstitution of manganese and cobalt oxyhydroxide mineral cores by the second method appears to mimic the naturally occurring process involving formation of the Fe(O)OH mineral core and provides an opportunity to compare similar oxyhydroxide mineral phases containing metals with different redox properties. In MOPS and AMPSO buffers, HoSF provides scaffolding for the constrained synthesis of these inorganic materials and plays an active role in controlling mineralization and preventing nonspecific bulk precipitation. We also observed that Tris was not as effective in forming mineral cores, possibly because it chelates Co(II) weakly[28] and thereby competes with HoSF to prevent proper core development. In the present study, kinetic and thermodynamic properties for the reduction of Co−HoSF and Mn−HoSF have been measured and are now compared with those of naturally occurring Fe−HoSF.

The chemical reaction of Fe(III)−HoSF with viologens, in the absence of chelators, rapidly and quantitatively produces HoSF with a stable $Fe(OH)_2$ mineral core as previously reported.[8] The reaction of Co(III)−HoSF with various viologen mediators is also rapid and quantitative, and the resulting $Co(OH)_2$−HoSF is stable for days as long as pH > 8.0 and O_2 is absent. The use of chemical reducing reagents with different redox potentials showed that the M(III)−HoSF mineral cores are readily reduced and established a reduction potential that was positive relative to that of AH_2. In contrast, the previously reported reduction potential for Fe(III)−HoSF was lower than that of AH_2 by approximately 150 mV, precluding reduction by ascorbic acid. These results indicate that the Co(III)−HoSF is a significantly stronger oxidant than Fe(III)−HoSF. Similar conclusions apply to Mn(III)−HoSF. Combining the results of reaction 1 with the corresponding reaction involving iron and taking into account the relative reduction potentials reported in this study, the Co(III)−HoSF should oxidize the Fe(II)−HoSF core as shown by

$$\text{Co(III)−HoSF} + \text{Fe(II)−HoSF} \rightarrow \text{Co(II)−HoSF} + \text{Fe(III)−HoSF} \quad (3)$$

This reaction was carried out as part of the present study and was observed to be rapid at pH 8.0. Also, because there is no net OH^- change, it should be independent of pH at values of pH > 7.0, where $Fe(OH)_2$ and $Co(OH)_2$ are stable. The fact that the reaction occurs presents some interesting mechanistic questions since electrons must transfer from one core to the other, presumably through the protein shell(s). Additionally, the rate and extent of reaction will depend on the structure and stability of the oxyhydroxide mineral cores. Thus, it should be possible to influence the reaction by changing the nature and/or stability of the mineral cores. Figure 2 shows that the Co(O)OH mineral core can be formed in the HoSF interior with different stabilities and properties, depending on the conditions used during reconstitution. This and other possibilities are under investigation in our laboratory.

As demonstrated above, Co− or Mn−HoSF not only oxidizes Fe(II)−HoSF, but also Fe^{2+} added to solution. This Fe^{2+} is oxidized and enters the ferritin core, displacing a portion of the Co or Mn that is already present. It seems likely that the less stable M(II) (M = Co or Mn) is the species that is displaced by the iron and leaves the core. However, not all of the M was released as ~20−30% remained associated with the mineral core and was either trapped or perhaps remained attached to the protein interior at nucleation sites, where the M(O)OH core was initially formed. An understanding of the relative stability of the different core materials, the rates of core formation, and the processes by which the cores are formed will be important to the development of methods to create novel types of mixed-metal cores.

In summary, the present work showed that HoSF containing cobalt or manganese oxyhydroxide mineral cores can

(27) Dominguez-Vera, J. M.; Colacio, E. *Inorg. Chem.* **2003**, *42*, 6983−6985.
(28) Good, N. E.; Winget, G. D.; Winter, W.; Connolly, T. N.; Izawa, S.; Singh, R. M. M. *Biochemistry* **1966**, *5*, 467−477.

be quantitatively reduced via a single electron reaction to form a stable $M(OH)_2$ mineral core, where M = Co or Mn. Reduction with AH_2 is an equilibrium process, which is first order in both AH_2 and Co−HoSF or Mn−HoSF. $Co(OH)_2$ and $Mn(OH)_2$ remain within the ferritin interior after reduction with AH_2 or other reductants in the absence of chelators. The cores in Co(III)−HoSF and Mn(III)−HoSF are moderately strong oxidants and are able to serve as the sole oxidant for the Fe deposition into the ferritin interior. When Fe^{2+} is used as the reductant, it is oxidized and deposited as Fe(O)OH within the ferritin interior, resulting in the release of 70−80% of the $M(OH)_2$ from the core.

Acknowledgment. This research was supported by Grant No. NCC-1-02005 from the National Aeronautics and Space Administration (NASA).

Supporting Information Available: Figure showing equilibrium constant determination for Co(O)OH−HoSF reduction by AH_2 (PDF). This material is available free of charge via the Internet at http://pubs.acs.org.

IC049085L